

# Microburst Nowcasting Applications of GOES

Kenneth L. Pryor  
Center for Satellite Applications and Research (NOAA/NESDIS)  
Camp Springs, MD

## 1. INTRODUCTION AND BACKGROUND

Recent testing and validation have found that the Geostationary Operational Environmental Satellite (GOES) microburst products are effective in the assessment and short-term forecasting of downburst potential and associated wind gust magnitude. Two products, the GOES sounder Microburst Windspeed Potential Index (MWPI) and a new two-channel GOES imager brightness temperature difference (BTD) product have demonstrated capability in downburst potential assessment (Pryor 2009; Pryor 2010). The GOES sounder MWPI algorithm is a predictive linear model developed in the manner exemplified in Caracena and Flueck (1988):

$$\text{MWPI} \equiv \{(\text{CAPE}/100)\} + \{\Gamma + (T - T_d)_{850} - (T - T_d)_{670}\}$$

where  $\Gamma$  is the lapse rate in degrees Celsius (C) per kilometer from the 850 to 670 mb level, and the quantity  $(T - T_d)$  is the dewpoint depression (C). In addition, it has been found recently that the BTD between GOES infrared channel 3 (water vapor,  $6.5\mu\text{m}$ ) and channel 4 (thermal infrared,  $11\mu\text{m}$ ) can highlight regions where severe outflow wind generation (i.e. downbursts, microbursts) is likely due to the channeling of dry mid-tropospheric air into the precipitation core of a deep, moist convective storm. Rabin et.al. (2010) noted that observations have shown that  $\text{BTD} > 0$  can occur when water vapor exists above cloud tops in a stably stratified lower stratosphere and thus,  $\text{BTD} > 0$  has been used a measure for intensity of overshooting convection. A new feature presented in this paper readily apparent in BTD imagery is a "dry-air notch" that signifies the channeling of dry air into the rear flank of a convective storm.

In addition, a comparison study between the GOES-R Convective Overshooting Top (OT) Detection and MWPI algorithms has been completed for cases that occurred during the 2007 to 2009 convective seasons over the southern Great Plains. The OT detection algorithm (Bedka et al. 2010) is a pattern recognition-based technique that employs brightness temperature (BT) data from the GOES thermal infrared channel. Output OT detection algorithm parameters include cloud top minimum BT and a BT difference between the overshooting top and surrounding convective anvil cloud. Favorable results of the comparison study include a statistically significant negative correlation between the OT minimum temperature and MWPI values and associated measured downburst wind gust magnitude. The negative functional relationship between the OT parameters and wind gust speed highlights the importance of updraft strength, realized by large CAPE, in the generation of heavy precipitation and subsequent intense convective downdraft generation. This paper will provide an updated assessment of the GOES MWPI and GOES BTD algorithms, presents case studies demonstrating effective operational use of the microburst products, and presents results of the intercomparison study of the GOES-R overshooting top (OT) detection algorithm over the United States Great Plains region.

## 2. METHODOLOGY

### 2.1 GOES Microburst Products

The objective of the validation effort should be to qualitatively and quantitatively assess and intercompare the performance of the MWPI and BTD algorithms by employing classical statistical analysis of real-time data. Accordingly, this effort entails a study of downburst events in a manner that emulates historic field projects such as the 1982 Joint Airport Weather Studies (JAWS) (Wakimoto 1985) and the 1986 Microburst and Severe Thunderstorm (MIST) project (Atkins and Wakimoto 1991). Algorithm output data was collected for downburst events that occur during the warm season (especially between 1 June and 30 September) and was validated against surface observations of convective wind gusts as recorded by reliable surface observation stations in mesoscale networks. Wakimoto (1985) and Atkins and Wakimoto (1991) discussed the effectiveness of using mesonet surface observations and radar reflectivity data in the verification of the occurrence of downbursts. Well-defined peaks in wind speed as well as significant temperature decreases (Wakimoto 1985; Atkins and Wakimoto 1991) were effective indicators of high-reflectivity downburst occurrence.

As illustrated in the flowchart in Figure 1, MWPI product images are generated by Man computer Interactive Data Access System (McIDAS)-X by a program that reads and processes GOES sounder data, calculates and collates microburst risk values, and overlays risk values on GOES imagery. Output images are then archived via FTP and HTTP to the GOES Microburst Products web page. For selected downburst events, the MWPI product was generated using the [Graphyte Toolkit](#). The MWPI algorithm, as implemented in the Graphyte Toolkit, reads and processes GOES sounder profile data in binary format available on the GOES sounding profile web page (<http://www.star.nesdis.noaa.gov/smcd/opdb/goes/soundings/html/sndbinary23L.html>). The MWPI is then calculated for each retrieval location and plotted as a colored marker on a user-defined map. Examples of Graphyte microburst algorithm output images are shown in Figures 2 and 4.

For the BTD product, image data consisted of derived brightness temperatures from GOES-East (GOES-12, 2009 and before; GOES-13, 2010 and after) 4-km resolution water vapor (band 3) and thermal infrared (band 4), obtained from the Comprehensive Large Array-data Stewardship System (CLASS, <http://www.class.ncdc.noaa.gov/>). Microburst algorithm output was visualized by McIDAS-V software (Available online at <http://www.ssec.wisc.edu/mcidas/software/v/>). A contrast stretch and built-in color enhancement ("Pressure") were applied to the output images to highlight patterns of interest including overshooting tops and dry-air notches. The dry -air notch identified in the BTD image is analogous in concept to the rear-inflow notch (RIN) as identified in radar imagery and documented in Przybylinski (1995). Next Generation Radar (NEXRAD) and Terminal Doppler Weather Radar (TDWR) base reflectivity imagery from National Climatic Data Center (NCDC) were utilized to verify that observed wind gusts are associated with high-reflectivity downbursts and not associated with other types of convective wind phenomena (i.e. gust fronts). An application of radar imagery is to infer microscale physical properties of downburst-producing convective storms. Particular radar reflectivity signatures, such as the rear-inflow notch (RIN)(Przybylinski 1995) and the spearhead echo (Fujita and Byers 1977), are effective indicators of the occurrence of downbursts.

Since surface data quality is paramount in an effective validation program, relatively flat, treeless prairie regions were chosen as study regions. The treeless, low-relief topography that dominates sparsely populated regions such as the U.S. High Plains allowed for the assumption of horizontal homogeneity when deriving a conceptual model of a boundary layer thermodynamic structure favorable for downbursts. More importantly, planar topography and water body surfaces facilitate relatively smooth flow (due to small surface roughness) with respect to downburst winds in which drag and turbulent eddy circulation resulting from surface obstructions (i.e., buildings, hills, trees) are minimized. Equation 4.6 in Sorbjan (1989) describes the wind profile in the surface layer and dictates that the relatively small roughness parameter of short grass prairie would permit wind gust measurements that are more representative of downburst intensity.

Over the eastern United States, coastal and estuarine waters would be optimal for a validation study. Observational data from Integrated Ocean Observing System (IOOS) stations (<http://www.ioos.gov/catalog/>) and WeatherFlow (<http://datascope.weatherflow.com/>) was preferred for algorithm validation. Especially noteworthy in mesonet station siting is the superior wind exposure that satisfies World Meteorological Organization (1983) standards and minimal slope in the vicinity of each station that reduces topographic effects that may influence downburst magnitude and resulting measured surface wind gusts. Shafer et al. (1993) addressed the preference of rural station siting to avoid anthropogenic factors, especially factors that may influence convective wind gust magnitude as recorded by mesonet stations. Site characteristics, data quality assurance, and wind sensor calibration are thoroughly documented in Brock et al. (1995) and Schroeder et al. (2005).

In order to assess the predictive value of the algorithm output, the closest representative index values were obtained for retrieval times one to three hours prior to the observed surface wind gusts. Representativeness of proximate index values was ensured by determining from analysis of surface observations, and radar and satellite imagery, that no change in environmental static stability and air mass characteristics between product valid time and time of observed downbursts had occurred. Furthermore, in order for the downburst observation to be included in a validation data set, it was required that the parent convective storm cell of each downburst, with radar reflectivity greater than 35 dBZ, be located nearly overhead at the time of downburst occurrence. An additional criterion for inclusion into a data set is a wind gust measurement of at least F0 intensity (35 knots) on the Fujita scale (Fujita 1971). Wind gusts of 35 knots or greater are considered to be operationally significant for transportation, especially boating and aviation. An algorithm devised by Wakimoto (1985) to visually inspect wind speed observations over the time intervals encompassing candidate downburst events should be implemented to exclude gust front events from the validation data set. In summary, the screening process employed to build the validation data set that consists of criteria based on surface weather observations and radar reflectivity data should yield a statistically significant sample size of downbursts and associated index values.

Covariance between the variables of interest, MWPI and surface downburst wind gust speed, was considered. Algorithm effectiveness was assessed as the correlation between MWPI values and observed surface wind gust velocities. Statistical significance testing was conducted to determine the confidence level of the correlation between observed downburst wind gust magnitude and microburst risk values. Examples of MWP and BTD algorithm validation employing the direct comparison method are shown graphically in Section 3.

## 2.2 GOES Overshooting Top Detection Algorithm

A comparison study between the GOES-R Convective Overshooting Top (OT) Detection and MWPI algorithms has also been completed for cases that occurred during the 2007 to 2009 convective seasons over the southern Great Plains. The OT detection algorithm (Bedka et al. 2010) is a pattern recognition-based technique that employs brightness temperature (BT) data from the GOES infrared window (IRW) channel. Dworak et al. (2011) describes the OT detection method as follows: (1) Relative BT minima that are lower than 215 K are first identified and then compared to an NWP tropopause temperature to verify that the pixels are indeed cloud tops “overshooting” through the tropopause region. (2) Checks are then performed to ensure that no minima are located within 15 km of each other so that portions of the same OT are not classified as two independent tops. (3) The IRW BT of the anvil cloud surrounding the potential OT is then sampled at an ~8 km radius in 16 directions and must have an IRW temperature at or colder than 225 K to be included in the mean computation. (4) At least 5 valid anvil pixels must be present to ensure that the anvil is of relatively large horizontal extent but allows an anvil to occupy as small as a 90° quadrant, which might be the case when strong jet-level winds are present. (5) A pixel is classified as an overshooting top if it is  $\geq 6.5$  K colder than the mean BT of the surrounding anvil cloud. Output OT detection algorithm parameters that include cloud top minimum BT and a BT difference between the overshooting top and surrounding convective anvil cloud have been compared to the closest representative MWPI values and closest measured downburst wind gusts by Oklahoma and West Texas Mesonet stations. Close correspondence between the location of overshooting tops, proximate MWPI values, and the location of observed downburst winds are evident in Figures 2, 3, and 12.

## 3. CASE STUDIES

### 3.1 August 2009 Oklahoma Downbursts

During the afternoon of 10 August 2009, strong convective storms developed along a cold front that extended from eastern Kansas to the Oklahoma Panhandle. The storms tracked eastward and produced several strong downbursts over northwestern and north-central Oklahoma during the late afternoon and evening. It was found that the GOES MWPI, BTD and OT detection algorithms were effective in indicating the intensity of convective storm activity and resulting downburst wind gust magnitude.

At 2100 UTC, Figure 2, the MWPI product image displayed elevated values widespread over Kansas and Oklahoma with high values (red) that indicate wind gust potential greater than 50 knots extending from northeastern to southwestern Oklahoma, well ahead of the developing convective storm activity. By 2200 UTC, MWPI values increased significantly downstream of a new area of developing storm activity along the cold front. An intrusion of dry mid-tropospheric air was becoming apparent on the western flank of the developing convective storm complex over the eastern Oklahoma Panhandle and extreme southern Kansas. Figure 2c, the Graphyte visualization of the 2200 UTC MWPI, shows moderate values (36 to 42, green markers) in the vicinity of Dodge City, Kansas (DDC), the location of the 0000 UTC radiosonde observation (RAOB) displayed in Figure 3. Figure 2c is also effective in highlighting that the Freedom downburst occurred in proximity to a local maximum in MWPI (near 60, red marker) just north of the Kansas-Oklahoma border. Dry air notches had become especially well-defined on the

northern and western flanks of the convective storm as shown in the 2332 UTC BTD image in Figure 3.

Note that in Figure 3, the overshooting top was co-located with a maximum in radar reflectivity and located 13 km northwest of the Freedom mesonet station, where a downburst wind gust of 64 knots was recorded between 2340 and 2345 UTC. The cold overshooting top BT value of 196K was associated with the severe downburst, highlighting the importance of convective storm updraft strength in the generation of severe weather, especially high winds. The closest representative MWPI value of 52 corresponded to wind gust potential of 50 to 64 knots. A dry air notch, apparent in the BTD image as a light-to-dark blue shaded indentation, illustrated the role and importance of the channeling of dry, mid-tropospheric air into the rear flank of the convective storm and the subsequent generation of intense downdrafts. The favorable environment for downbursts was well illustrated in the 0000 UTC (11 August) radiosonde observation from Dodge City, Kansas. Large CAPE and a large temperature lapse rate below the 550-mb level definitely were instrumental in fostering strong storm updrafts that was realized as a heavy precipitation core and overshooting top observed at 2332 UTC. In addition, the sounding indicated the presence of two prominent dry-air layers centered near the 400-mb and 700-mb levels. Strong westerly winds of 40 to 50 knots were measured in the upper dry-air layer that likely injected this dry air into the storm precipitation core that enhanced downdraft acceleration and subsequent severe winds observed on the surface by the Freedom mesonet station. All of these favorable conditions were reflected in the 2332 UTC BTD image that displayed concurrent high storm radar reflectivity, an overshooting top, and a prominent dry-air notch on the western flank of the storm.

### **3.2 August 2010 DC-Maryland Downbursts**

During the afternoon of 5 August 2010, strong convective storms developed over western Maryland and Virginia ahead of a cold front and produced downburst winds as observed by NOAA Chesapeake Bay Interpretive Buoy System (CBIBS) and Physical Oceanographic Real-Time System (PORTS) stations. The 1900 and 2000 UTC MWPI product images on 5 August effectively indicated the potential for strong downbursts over the tidal Potomac River and Chesapeake Bay regions during the late afternoon, with wind gust potential of 35 to 49 knots. Wind gusts of 42 knots were recorded by CBIBS and PORTS stations in the Washington, DC metropolitan area near 2000 UTC, followed by a 40-knot gust recorded about an hour later over the Chesapeake Bay. These storms posed a significant threat in the form of “knockdown” winds to sailing vessels operating in the tidal Potomac River and middle Chesapeake Bay.

Figure 4 shows the 1900 and 2000 UTC MWPI product images that indicated elevated wind gust potential (35 to 49 knots, yellow index values in McIDAS image) in proximity to the location of downburst wind gusts recorded by CBIBS buoys (“UP”, “G”) one hour prior to each event. The 1900 UTC MWPI image shows strong thunderstorms developing along a cold front that extended from northern New Jersey to western Virginia. By 2000 UTC, the MWPI displayed a strong thunderstorm over the Washington, DC metropolitan area near the time 42-knot wind gusts were recorded at the Washington PORTS station and Upper Potomac (“UP”) buoy. One hour later, another strong downburst wind gust of 40 knots was recorded at Gooses Reef (“G”) buoy in the Chesapeake Bay. The Graphyte visualizations of the MWPI also shown in Figure 4 (b, d) emphasized that, similar to the August 2009 case, the strongest downburst winds occurred near local maxima in index values indicated by yellow markers in the

Washington DC area (Figure 4b) and an orange marker over the western Delmarva Peninsula (Figure 4d). As shown in Figure 5, the pre-convective environment over the Washington, DC area was characterized by strong instability that resulted from the presence of large CAPE, a dry sub-cloud layer, and a steep temperature lapse rate below the 700-mb level. Note the presence of a well-defined dry-air layer above the 500-mb level. This indicates the availability of dry air in the mid-troposphere for the production of strong downdraft energy that was effectively displayed in GOES BTD imagery.

Figure 6 shows that well-defined dry air notches were displayed by BTD product imagery as light to dark blue-shaded indentations on the western and northwestern flanks of the convective storms. The dry-air notches on the rear flank of the storm moving over the Washington, DC area and then over the middle Chesapeake Bay signified the channeling of mid-tropospheric dry air into the storm precipitation core, providing the initial energy for strong convective downdrafts. Note that in general, the notches were oriented toward the southeast. High wind gusts recorded in the Washington, DC area and at Gooses Reef buoy were associated with a northwesterly wind direction, suggesting that momentum generated by the intrusion of dry air into the convective storm resulted in the strong downburst winds.

### **3.3 May 2011 Hampton Roads Downbursts**

During the afternoon of 24 May 2011, a multicellular convective storm developed over the southern piedmont of Virginia and tracked rapidly eastward toward the lower Chesapeake Bay. Between 2000 and 2100 UTC, as the convective storm passed over the Hampton Roads, one of the busiest waterways in the continental U.S., numerous severe wind gusts were recorded by WeatherFlow and Physical Oceanographic Real-Time System (PORTS) observing stations. After inspecting satellite and radar imagery for this event, it was apparent that these severe wind observations were associated with downburst activity. GOES MWPI imagery in Figure 7 indicated a general increase in wind gust potential over the Hampton Roads area during the afternoon hours, between 1900 and 2000 UTC. The increase in both convective and downdraft instability was reflected in the Norfolk, Virginia GOES sounding profile in Figure 8 as a marked increase in CAPE and an elevation and increasing amplitude of the mid-tropospheric dry-air layer. By 2000 UTC, the MWPI product indicated the highest wind gust potential, up to 64 knots, over Hampton Roads, where wind gusts of 57 to 63 knots were recorded by WeatherFlow and PORTS stations during the following hour. Visible imagery emphasized the multicellular structure of the storm with overshooting tops identifying the most intense convective cells that were capable of producing severe downbursts.

The first downburst wind gust of 53 knots was recorded at Poquoson WeatherFlow station (“P”) at 2011 UTC, followed by wind gusts of 57 knots at the Monitor-Merrimack Memorial Bridge-Tunnel (“M”, WeatherFlow), 59 knots at Hampton Flats (WeatherFlow), and 63 knots at Willoughby Degaussing Station (“W”, PORTS) between 2017 and 2020 UTC. Figure 9 illustrates the observing network over the Hampton Roads area that revealed the divergent nature of the downburst winds as the storm was tracking overhead. The GOES MWPI at 2000 UTC, overlying enhanced water vapor imagery in Figure 9a, and Figure 10a, the BTD product image at 2025 UTC, with overlying radar reflectivity, revealed favorable conditions for severe downbursts with prominent dry-air notches on the southwestern and northwestern flanks of the storm pointing toward the convective precipitation core. This signifies that the entrained mid-tropospheric dry air was interacting with the storm precipitation core to result in

evaporational cooling, negative buoyancy generation, and subsequent acceleration of storm downdrafts. Similar to the August 2010 case, GOES sounding profiles reflected elevated MWPI values by displaying the presence of large CAPE, a dry sub-cloud layer, and a steep temperature lapse rate below the 700-mb level. By 2040 UTC, as shown in Figure 10b, dry-air notches had become more pronounced in BTD imagery while prominent spearhead echoes were apparent in overlying radar imagery. Near this time, significant severe downburst winds were recorded by PORTS and WeatherFlow stations (“1I”, “3I”) on the Chesapeake Bay Bridge-Tunnel between Virginia Beach and Cape Charles. Downburst wind gusts of 67 knots and 62 knots were recorded at the First Island (“1I”) and Third Island (“3I”) observing stations, where spearhead echoes embedded in the convective storm were oriented toward each respective station. As the storm moved eastward over the Virginia Beach oceanfront, weaker downburst winds (47 knots at Sandbridge station, not shown) were recorded where wind gust potential of 35 to 49 knots was indicated at 2000 UTC. Graphyte visualizations were not shown for this case due to the lack of data plots over the Hampton Roads area.

#### **4. STATISTICAL ANALYSIS AND DISCUSSION**

Validation results for the 2007 to 2010 convective seasons have been completed for the MWPI and imager microburst products. GOES sounder-derived MWPI values have been compared to mesonet observations of downburst winds over Oklahoma and Texas for 208 events between June 2007 and September 2010. The correlation between MWPI values and measured wind gusts was determined to be .62 and was found to be statistically significant near the 100% confidence level, indicating that the correlation represents a physical relationship between MWPI values and downburst magnitude and is not an artifact of the sampling process. Figure 11 shows a scatterplot of MWPI values versus observed downburst wind gust speed as recorded by mesonet stations in Oklahoma and Texas. The MWPI scatterplot identifies two clusters of values: MWPI values less than 50 that correspond to observed wind gusts of 35 to 50 knots, and MWPI values greater than 50 that correspond to observed wind gusts of greater than 50 knots. The scatterplot illustrates the effectiveness of the MWPI product in distinguishing between severe and non-severe convective wind gust potential.

The comparison study between the GOES-R Convective Overshooting Top (OT) Detection and MWPI algorithms has also produced favorable results that include a statistically significant negative correlation between the OT minimum temperature and MWPI values and associated measured downburst wind gust magnitude, as shown in Figure 12. The negative functional relationship between the OT parameters and wind gust speed highlights the importance of updraft strength, realized by large CAPE, in the generation of heavy precipitation and subsequent intense convective downdraft generation.

Figure 12 shows the comparison of scatterplots of convective overshooting top (OT) minimum brightness temperature (BT) vs. GOES Microburst Windspeed Potential Index (MWPI) values (12c) and OT minimum BT vs. measured downburst wind gust speed (12d) for 47 cases that occurred between 2007 and 2009. A correlation of -0.39 was found between OT minimum BT and measured downburst wind gust speeds as recorded by Oklahoma and West Texas Mesonet stations. An even stronger negative correlation, -0.47 was found between OT minimum BT and co-located MWPI values for 47 downburst events. These statistically significant negative functional relationships indicate the importance of convective available potential energy (CAPE) in the generation of heavy precipitation cores in convective storms.

The resultant precipitation loading, as well as phase change cooling processes, foster the generation of negative buoyancy that accelerates a convective storm downdraft, eventually producing strong downburst winds upon impact on the surface. These results are consistent with the findings of Dworak et al. (2011) that show near linear relationship between overshooting top BT and magnitude and severe wind frequency (Figure 12a, b).

## 5. SUMMARY AND CONCLUSIONS

As documented in Pryor (2009, 2010), and proven by statistical analysis, the GOES sounder MWPI product has demonstrated capability in the assessment of wind gust potential over the southern Great Plains and Chesapeake Bay regions. Case studies and statistical analysis for downburst events that occurred during the 2007 to 2010 convective seasons demonstrated the effectiveness of the GOES microburst products. However, as noted by Caracena and Flueck (1988), the majority of microburst days during JAWS were characterized by environments intermediate between the dry and wet extremes (i.e. hybrid). As noted in Pryor (2009), the MWPI product is especially useful in the inference of the presence of intermediate or “hybrid” microburst environments, especially over the Great Plains region. Further validation over the Chesapeake Bay region should strengthen the functional relationship between MWPI values and downburst wind gust magnitude.

The dry-air notch identified in all three case studies presented above most likely represents drier (lower relative humidity) air that is channeled into the rear of convective storms and interacts with the precipitation cores, subsequently providing the energy for intense downdrafts and resulting downburst winds. Comparison of BTD product imagery to corresponding radar imagery revealed a correlation between the dry-air notch and the RIN. Entrainment of drier mid-tropospheric air into the precipitation core of the convective storm typically results in evaporation of precipitation, the subsequent cooling and generation of negative buoyancy (sinking air), and resultant acceleration of a downdraft. When the intense localized downdraft reaches the surface, air flows outward as a downburst. Ellrod (1989) noted the importance of low mid-tropospheric (500 mb) relative humidity air in the generation of the severe Dallas-Fort Worth, Texas microburst in August 1985. Thus, the channel 3-4 BTD product can serve as an effective supplement to the GOES sounder MWPI product. Further validation of the imager microburst product and quantitative statistical analysis to assess product performance will serve as future work in the development and evolution of the GOES microburst products.

## 6. REFERENCES

- Atkins, N.T., and R.M. Wakimoto, 1991: Wet microburst activity over the southeastern United States: Implications for forecasting. *Wea. Forecasting*, **6**, 470-482.
- Bedka, K., J. Brunner, R. Dworak, W. Feltz, J. Otkin, and T. Greenwald, 2010: Objective Satellite-Based Detection of Overshooting Tops Using Infrared Window Channel Brightness Temperature Gradients. *J. Appl. Meteor. Climatol.*, **49**, 181–202.



Brock, F. V., K. C. Crawford, R. L. Elliott, G. W. Cuperus, S. J. Stadler, H. L. Johnson and M. D. Eilts, 1995: The Oklahoma Mesonet: A technical overview. *Journal of Atmospheric and Oceanic Technology*, **12**, 5-19.

Caracena, F., and J.A. Flueck, 1988: Classifying and forecasting microburst activity in the Denver area. *J. Aircraft*, **25**, 525-530.

Dworak, R., K. M. Bedka, J. Brunner, and W. Feltz, 2011: Comparison between GOES-12 overshooting top detections, WSR-88D radar reflectivity, and severe storm reports. Submitted to *Wea. Forecasting*.

Ellrod, G. P., 1989: Environmental conditions associated with the Dallas microburst storm determined from satellite soundings. *Wea. Forecasting*, **4**, 469-484.

Fujita, T.T., and H.R. Byers, 1977: Spearhead echo and downburst in the crash of an airliner. *Mon. Wea. Rev.*, **105**, 129-146.

Pryor, K.L., 2009: Microburst windspeed potential assessment: progress and recent developments. [arXiv:0910.5166v3](https://arxiv.org/abs/0910.5166v3) [physics.ao-ph]

Pryor, K. L., 2010: Recent developments in microburst nowcasting using GOES. Preprints, 17th Conference on Satellite Meteorology and Oceanography, Annapolis, MD, Amer. Meteor. Soc.

Przybylinski, R.W., 1995: The bow echo. Observations, numerical simulations, and severe weather detection methods. *Wea. Forecasting*, **10**, 203-218.

Rabin, R., P. Bothwell, and S. Weiss, 2010: Temperature deviation from Equilibrium Temperature: Convective Overshoot from Satellite Imagery. [Available online at <http://overshoot.nssl.noaa.gov/>.]

Schroeder, J.L., W.S. Burgett, K.B. Haynie, I. Sonmez, G.D. Skwira, A.L. Doggett, and J.W. Lipe, 2005: The West Texas Mesonet: A technical overview. *Journal of Atmospheric and Oceanic Technology*, **22**, 211-222.

Wakimoto, R.M., 1985: Forecasting dry microburst activity over the high plains. *Mon. Wea. Rev.*, **113**, 1131-1143.

## **Acknowledgements**

The author thanks the [Oklahoma Mesonet](#), and Jay Titlow (WeatherFlow) for the surface weather observation data used in this research effort. The author thanks Michael Grossberg and Paul Alabi (NOAA/CREST, CCNY) for their implementation of the MWPI program into the Graphyte Toolkit and their assistance in generating the MWPI product images. The author also thanks Jaime Daniels (NESDIS) for providing GOES sounding retrievals displayed in this paper.

## Microburst Windspeed Potential Index Top Level Flowchart

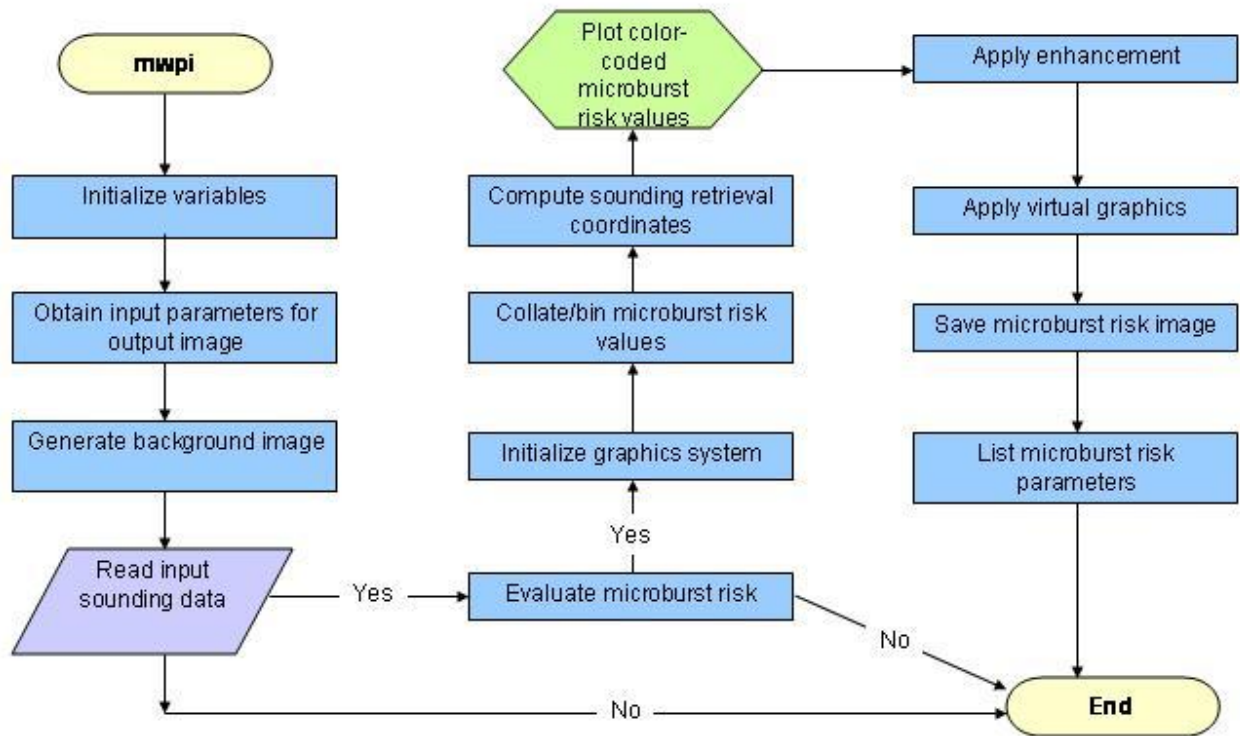


Figure 1. Flowchart illustrating the operation of the MWPI program.

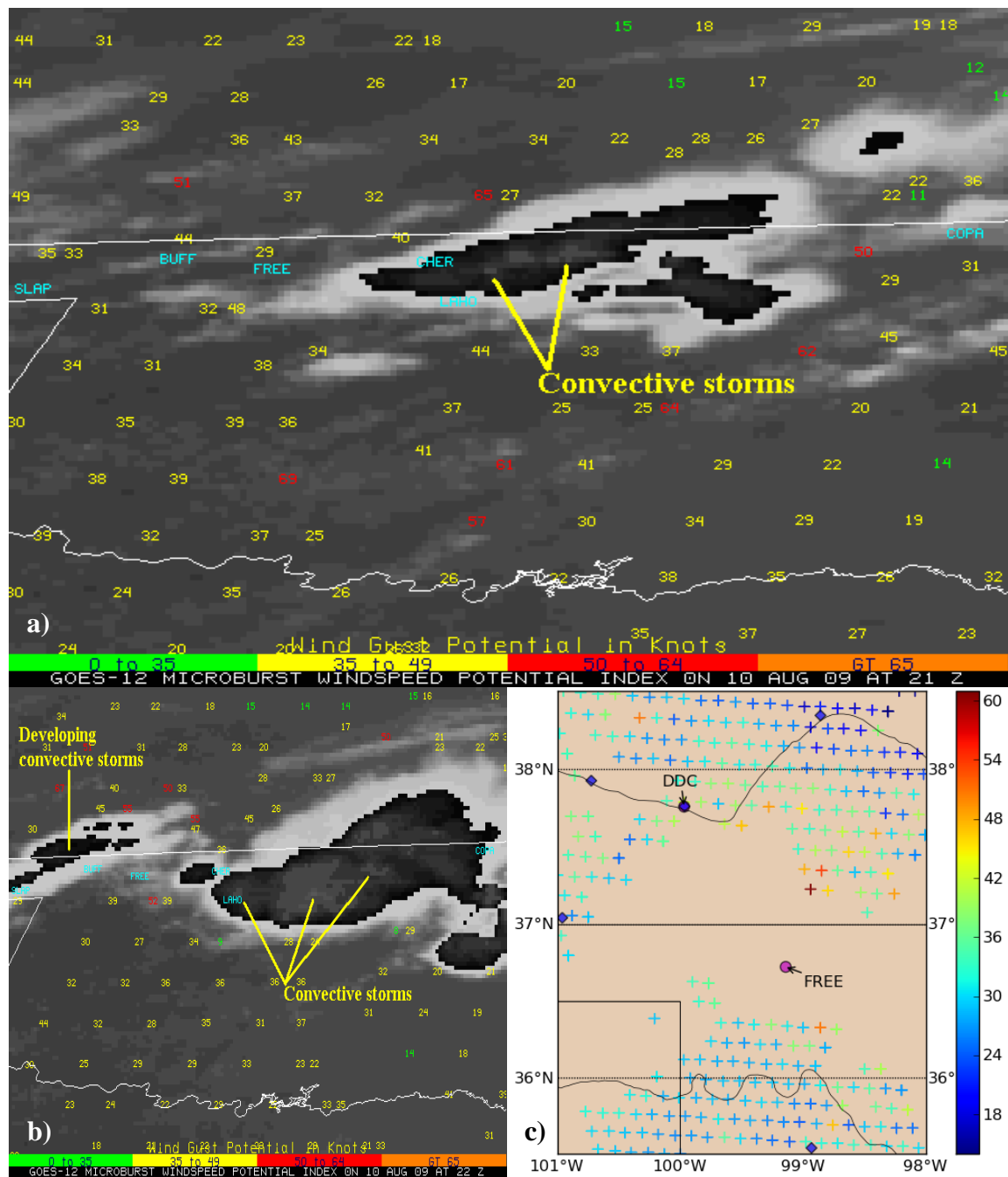


Figure 2. Geostationary Operational Environmental Satellite (GOES) Microburst Windspeed Potential Index (MWPI) on 10 August 2009 at a) 2100 UTC, b) 2200 UTC (McIDAS version), and c) 2200 UTC (Graphyte version).

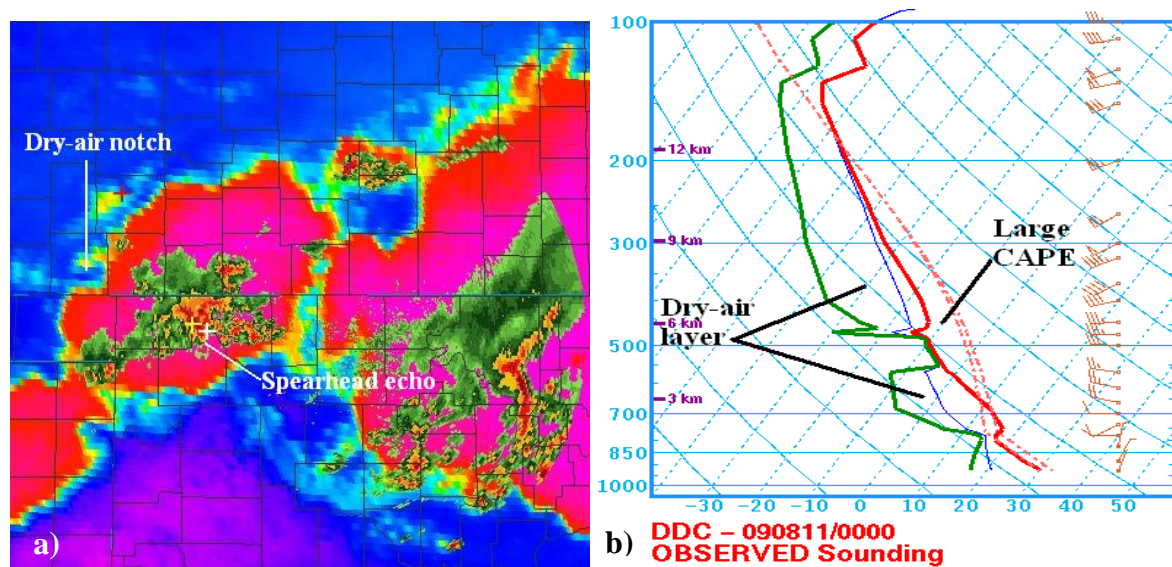


Figure 3. a) GOES imager channel 3-4 BTDR product at 2332 UTC 10 August 2009, with overlying radar reflectivity from Vance AFB NEXRAD; b) Radiosonde observation (RAOB) over Dodge City, Kansas (red cross) at 0000 UTC 11 August 2009. The location of downburst occurrence at Freedom, Oklahoma Mesonet station is marked with a white cross. The adjacent overshooting top, as indicated by the Bedka algorithm, is marked with a yellow cross.

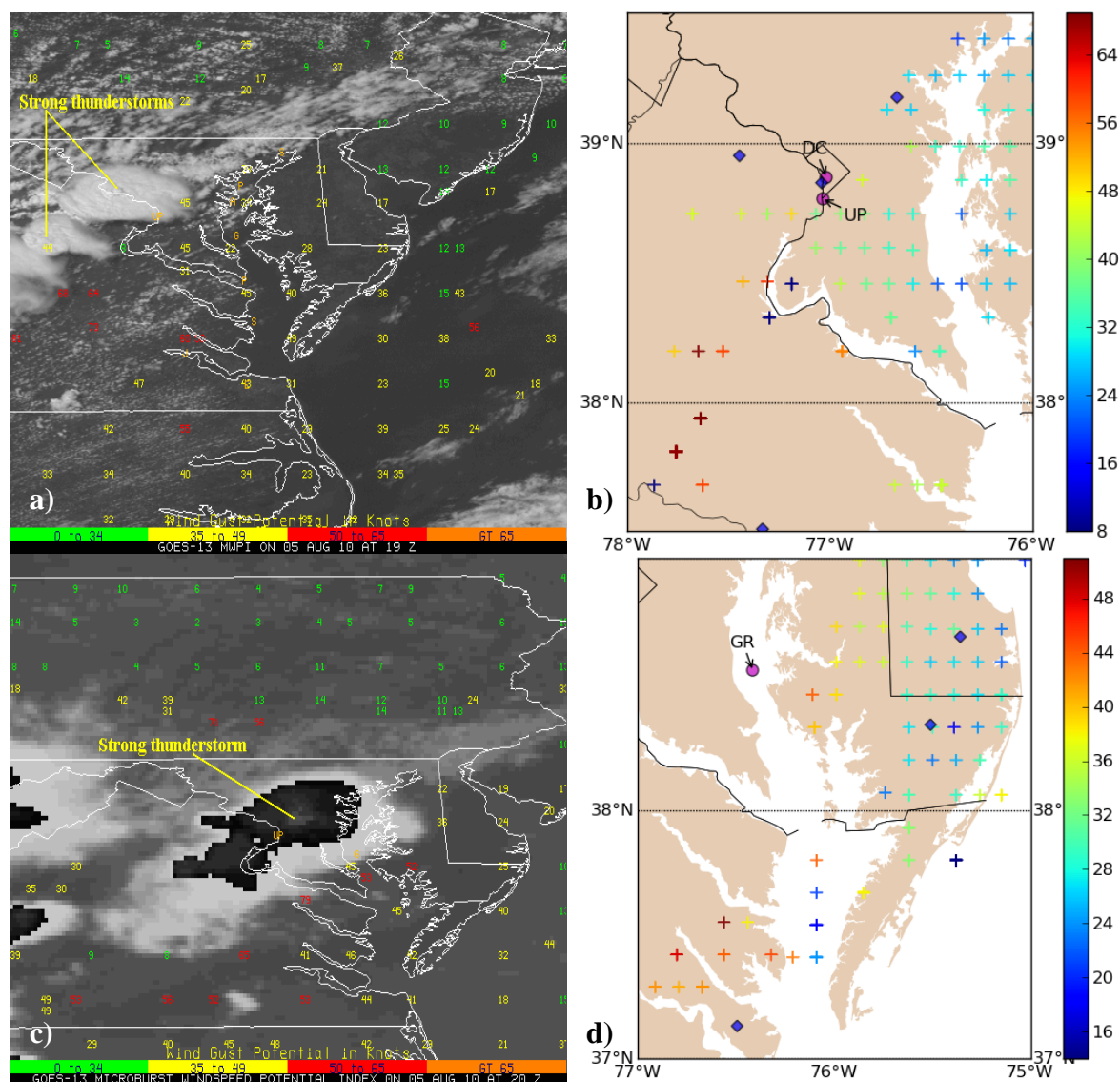


Figure 4. Geostationary Operational Environmental Satellite (GOES) MWPI product images at 1900 UTC 5 August 2010: a) McIDAS version, b) Graphyte version, and at 2000 UTC: c) McIDAS version, d) Graphyte version. The locations of the observation of downburst winds at Upper Potomac ("UP") and Gooses Reef (G) buoys are plotted on the images.

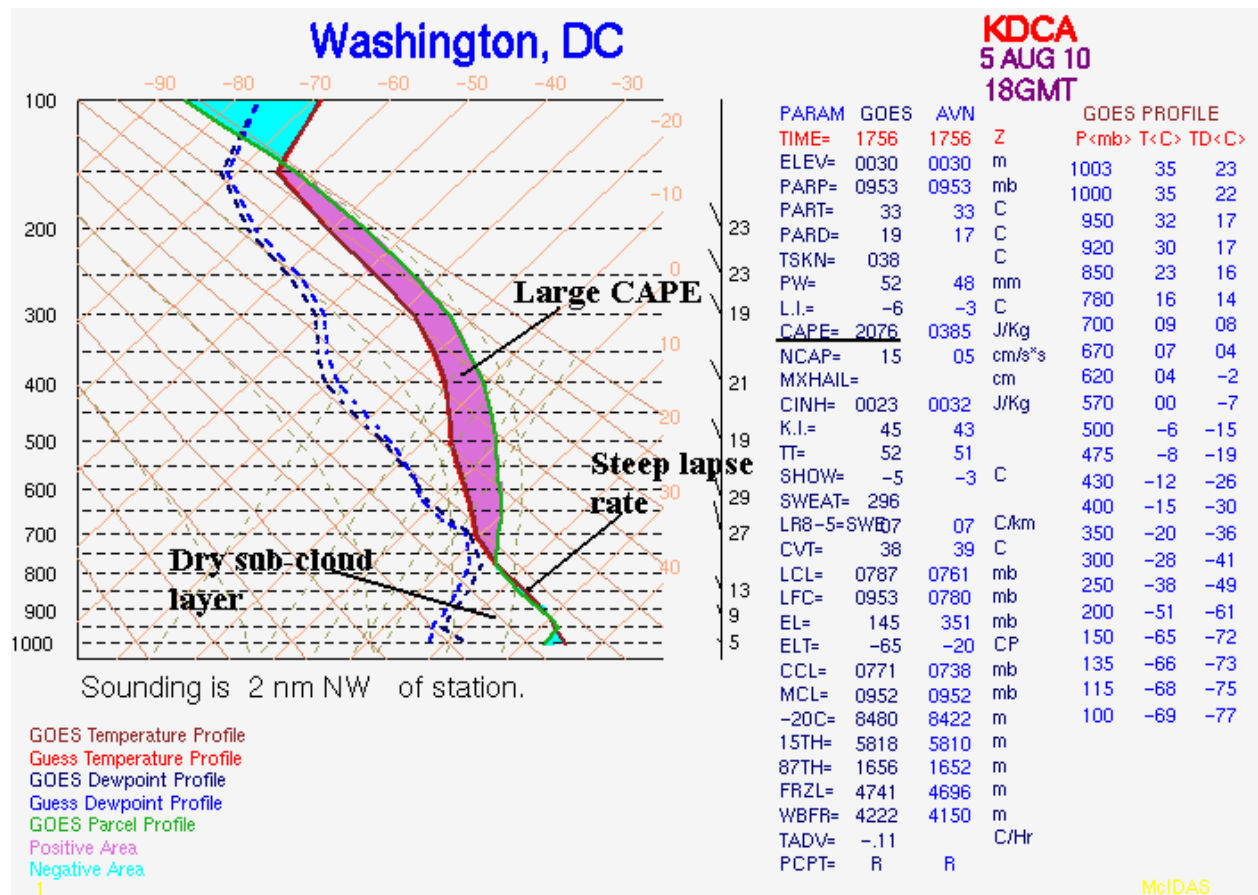


Figure 5. GOES sounding profile at 1800 UTC 5 August 2010 at Washington, DC.



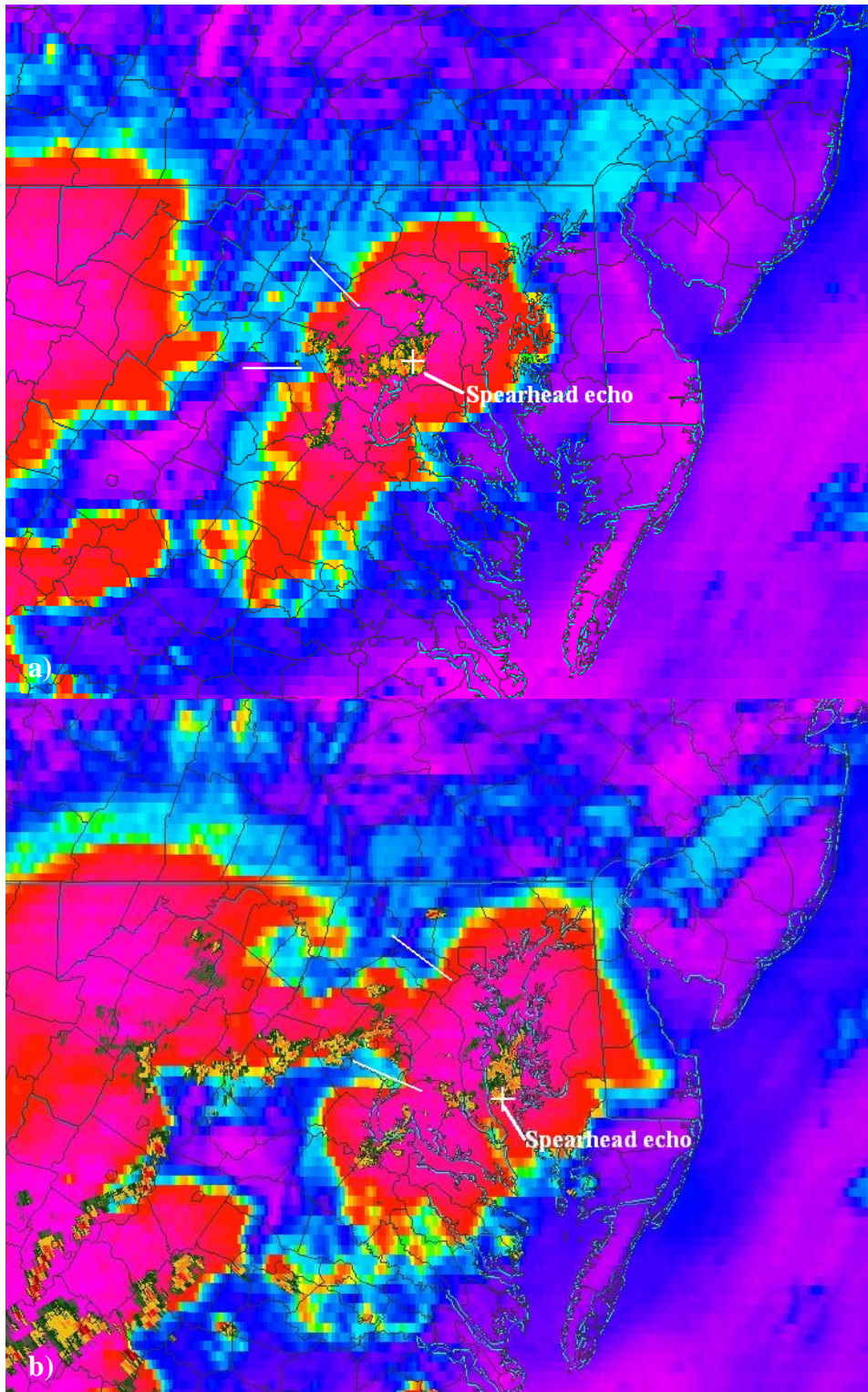


Figure 6. GOES imager channel 3-4 BTDR products at a) 1955 UTC and b) 2040 UTC 5 August 2010 with overlying radar reflectivity from Andrews Air Force Base TDWR. White crosses mark the location of the Upper Potomac buoy (a) and Gooses Reef buoy (b). White lines indicate the presence of dry-air notches.

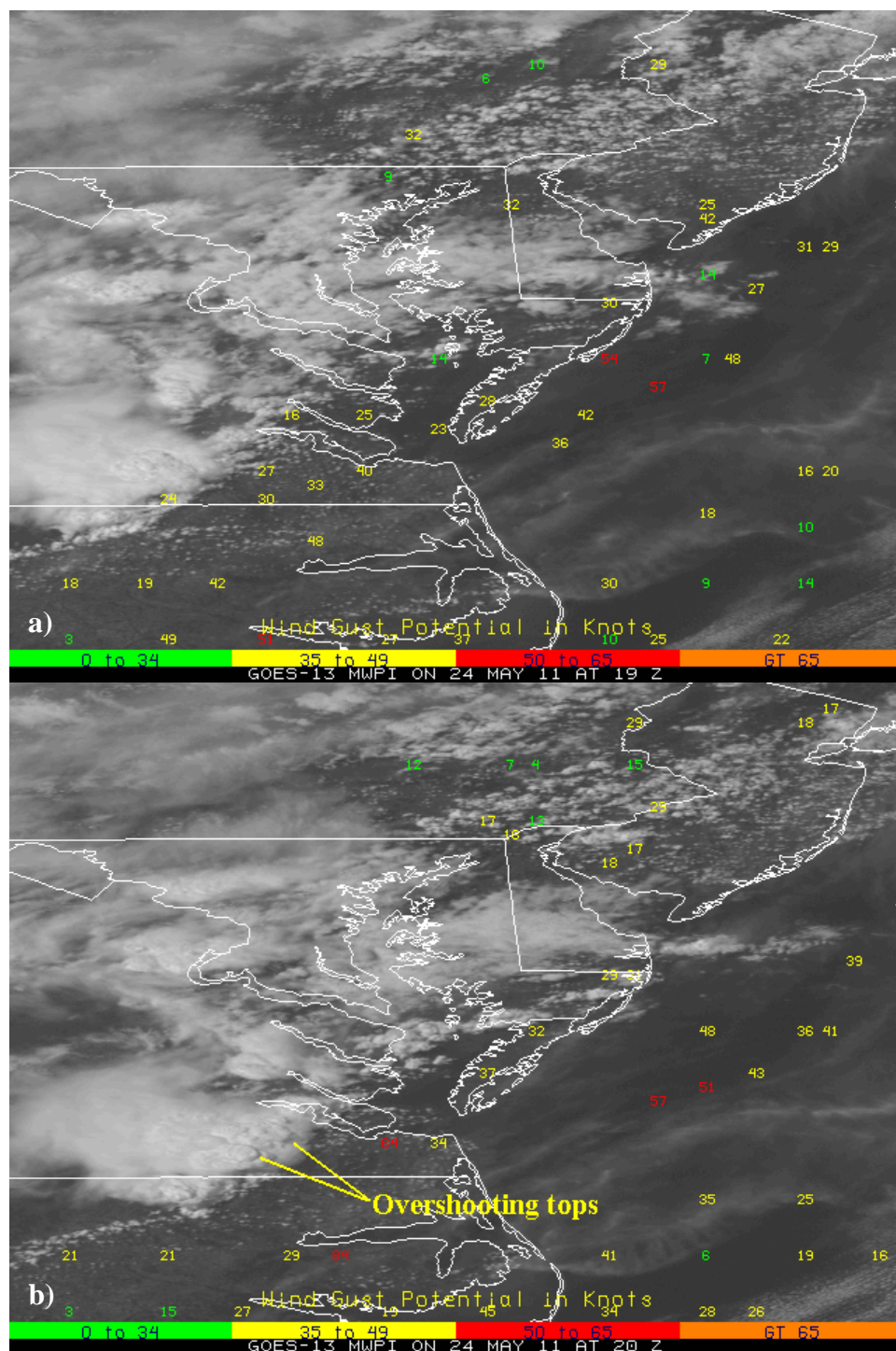


Figure 7. GOES MWPI product images at a) 1900 UTC and b) 2000 UTC 24 May 2011 overlying visible satellite imagery. A general increase in index values and associated downburst wind gust potential over Hampton Roads is apparent while the multicellular convective storm intensified on its track toward the lower Chesapeake Bay.



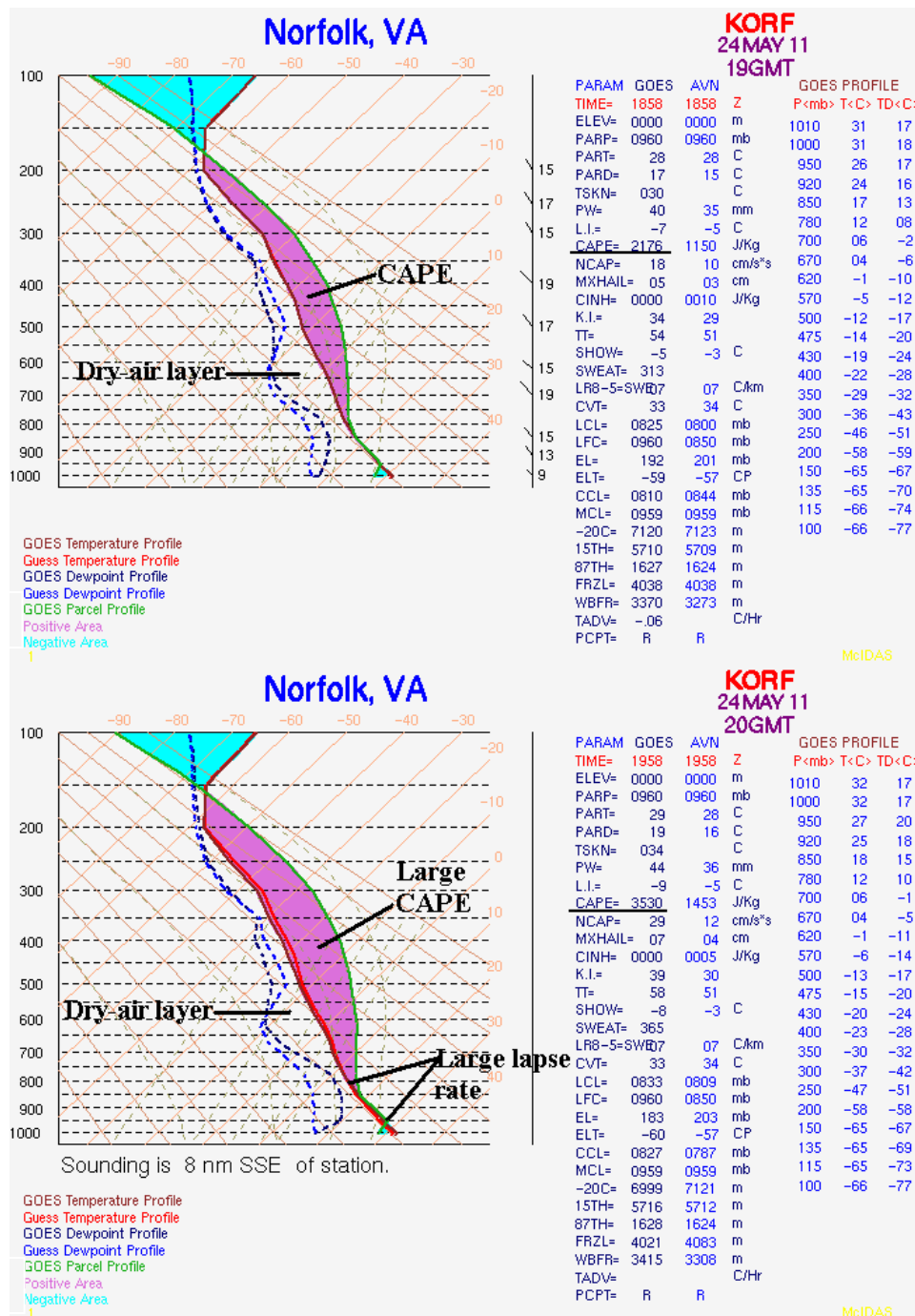


Figure 8. GOES sounding profiles over Norfolk, Virginia at a) 1900 UTC and b) 2000 UTC 24 May 2011.

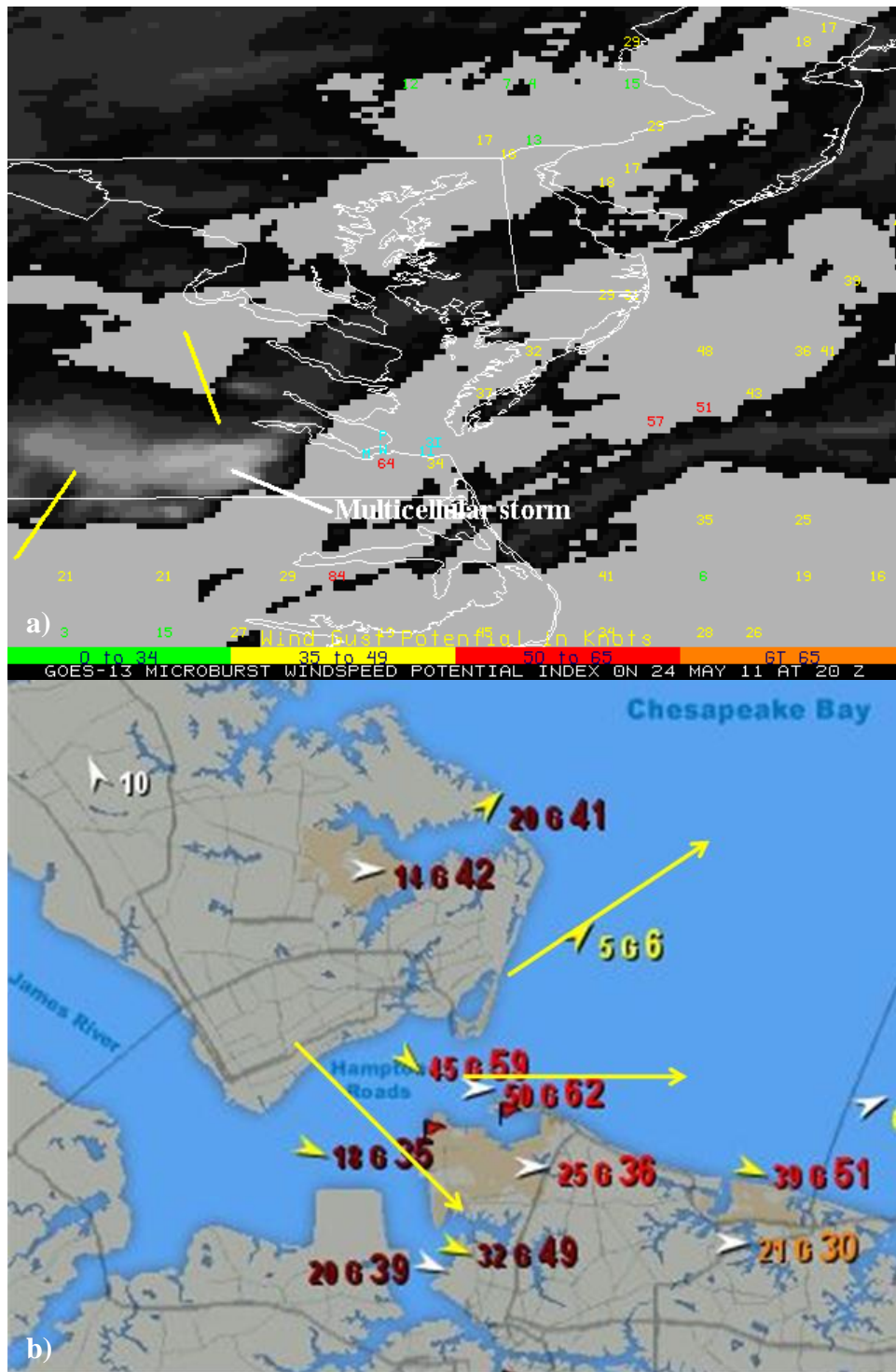


Figure 9. a) GOES MWPI product at 2000 UTC 24 May 2011 with index values overlying enhanced water vapor imagery, and b) WeatherFlow surface observation plot at 2037 UTC 24 May 2011 showing the divergent nature of convective storm outflow winds over Hampton Roads area. “M”, “H”, “P”, “1I”, and “3I” represent the locations of WeatherFlow and PORTS observations of downburst winds in a).

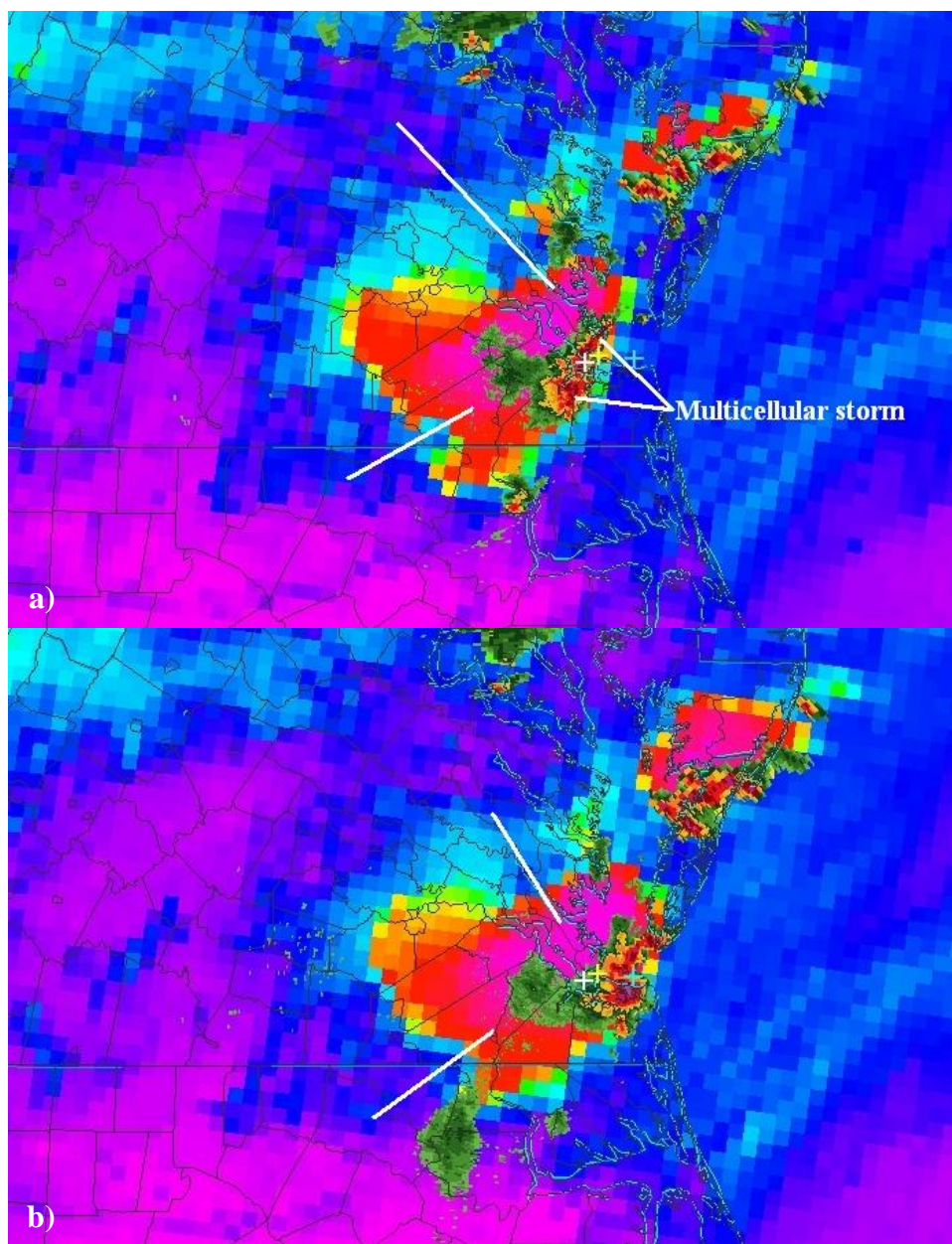


Figure 10. GOES imager channel 3-4 BTD products at a) 2025 UTC and b) 2040 UTC 24 May 2011 with overlying radar reflectivity from Wakefield, Virginia NEXRAD. White, yellow, and blue crosses mark the location of the Monitor-Merrimac Memorial Bridge-Tunnel, Willoughby Degaussing Station, and Chesapeake Bay Bridge-Tunnel observing stations, respectively. White lines indicate the presence of dry-air notches.

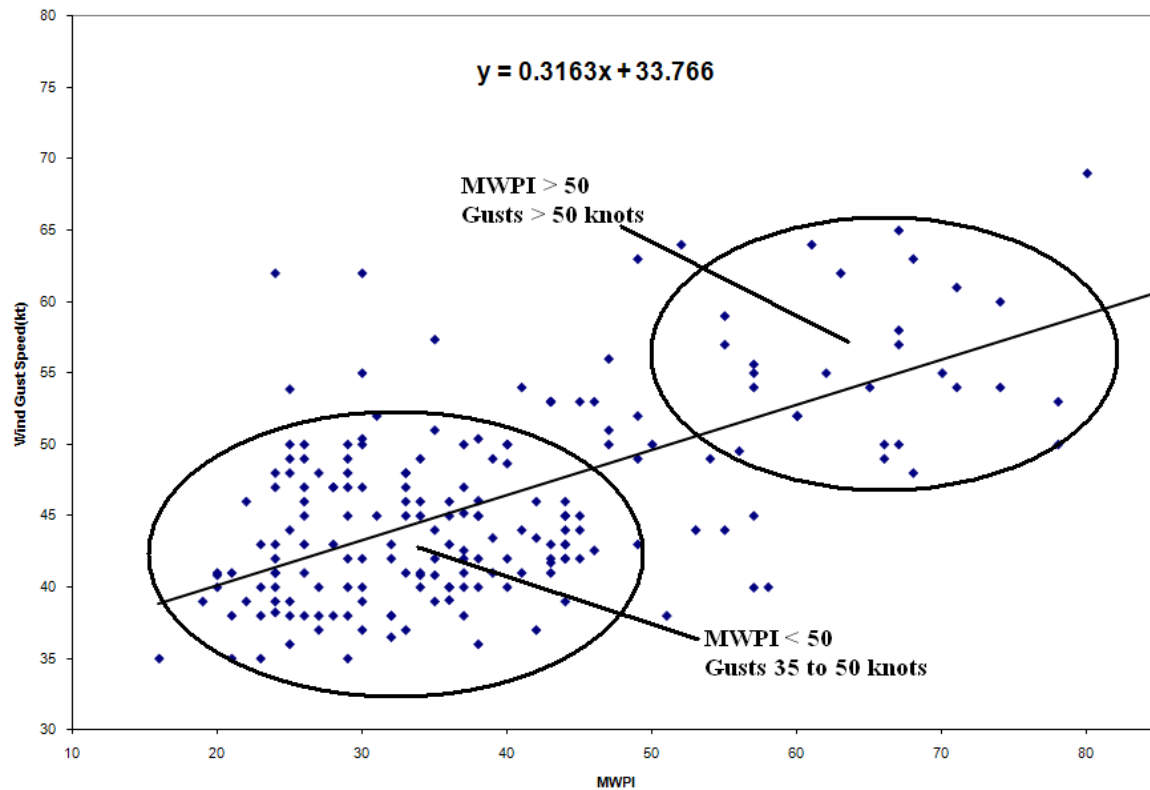


Figure 11. Statistical analysis of validation data over the Oklahoma and western Texas domain between June and September 2007 through 2010: Scatterplot of MWPI values vs. measured convective wind gusts for 208 downburst events.

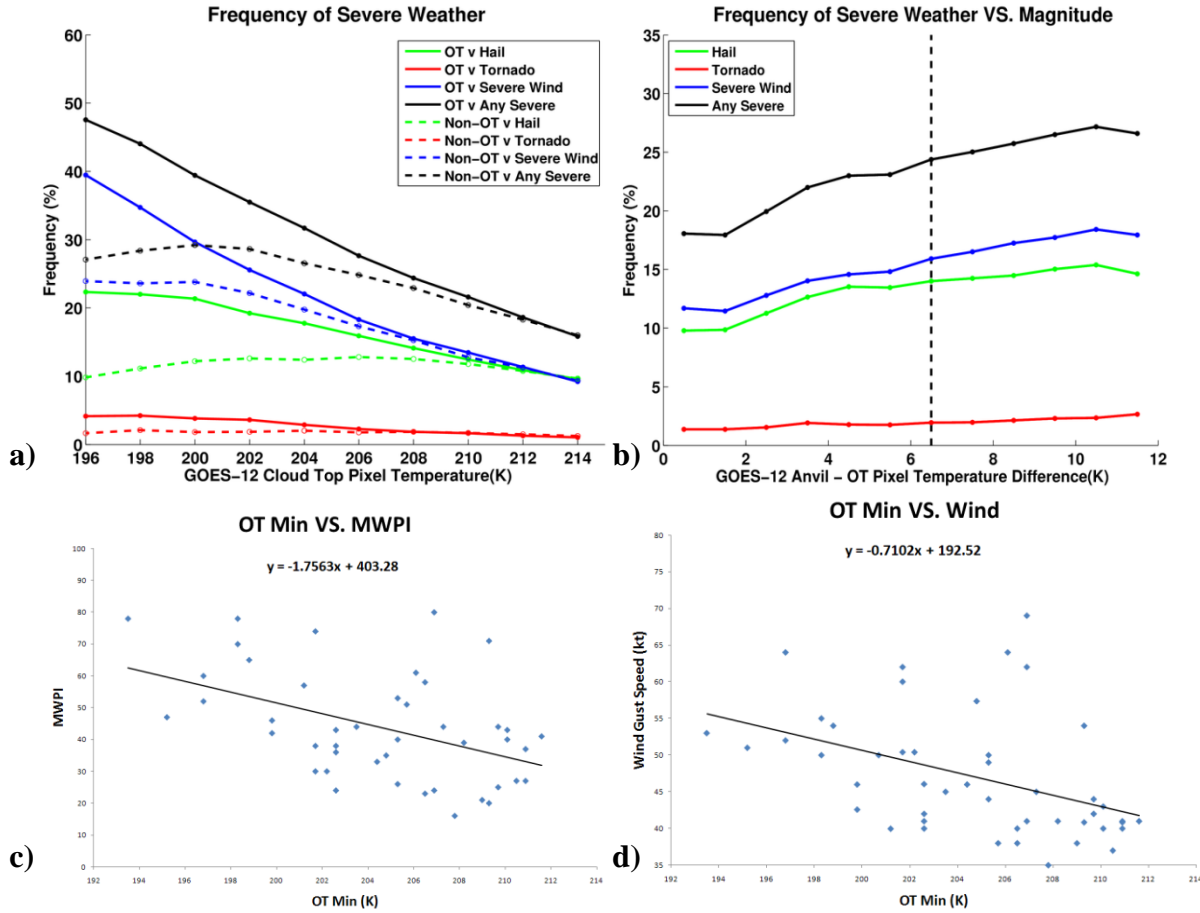


Figure 12. a) The frequency of severe weather for OTs (solid lines) and non-OT cold pixels (dashed lines) with varying IRW BT for each of the severe weather categories during the 2004-2009 warm seasons. b) Frequency of severe weather with varying BT difference between a pixel and the mean surrounding anvil temperature for each of the severe weather categories. The dashed line delineates the 6.5 K criteria required for a pixel to be considered an OT. c) Comparison of scatterplots of convective overshooting top (OT) minimum brightness temperature (BT) vs. GOES Microburst Windspeed Potential Index (MWPI) values and d) OT minimum BT vs. measured downburst wind gust speed (bottom) for 47 cases that occurred between 2007 and 2009.